Targeted Nanostructured Lipid Carrier Containing Galangin as a Promising Adjuvant for Improving Anticancer Effects of Chemotherapeutic Agents

Hamed Hajipour
Baqiyatallah University of Medical Sciences
Mohammad Nouri
Tabriz University of Medical Sciences
Marjan Ghorbani
Tabriz University of Medical Sciences
Ali Bahramifar
Baqiyatallah University of Medical Sciences
Reza Zolfaghari Emameh
National Institute for Genetic Engineering and Biotechnology
Ramezan Ali Taheri (taheri@bmsu.ac.ir)
Baqiyatallah University of Medical Sciences https://orcid.org/0000-0002-7391-276X

Research Article

Keywords: Galangin, cancer treatment, nanostructured lipid carrier, RGD

Posted Date: June 17th, 2021

DOI: https://doi.org/10.21203/rs.3.rs-600166/v1

Abstract

Purpose

Resistance to chemotherapeutic drugs is the main limitation of cancer therapy. The combination use of anticancer agents and Galangin (a naturally active flavonoid) amplifies the effectiveness of cancer treatment. This study aimed to prepare Arginyl-glycyl-aspartic acid (RGD) containing nanostructured lipid carrier (NLC-RGD) to improve the bioavailability of Galangin and explore its ability in improving the anti-cancer effects of doxorubicin (DOX).

Methods

Galangin loaded-NLC-RGD was prepared by hot homogenization method and characterized by diverse techniques. Then, cytotoxicity, uptake, and apoptosis induction potential of prepared nanoparticles beside the DOX were evaluated. Finally, the expression level of some ABC transporter genes was evaluated in Galangin loaded-NLC-RGD treated cells.

Results

Nanoparticles with appropriate characteristics of the delivery system (size: 120 nm, PDI: 0.23, spherical morphology, and loading capacity: 59.3 mg/g) were prepared. Uptake experiments revealed that NLC-RGD promotes the accumulation of Galangin into cancerous cells by integrin-mediated endocytosis. Results also showed higher cytotoxicity and apoptotic effects of DOX + Galangin loaded-NLC-RGD in comparison to DOX + Galangin. Gene expression analysis demonstrated that Galangin loaded-NLC-RGD downregulates ABCB1, ABCC1, and ABCC2 more efficiently than Galangin.

Conclusion

These findings indicated that delivery of Galangin by NLC-RGD makes it an effective adjuvant to increase the efficacy of chemotherapeutic agents in cancer treatment.

1. Introduction

Despite the persistent advancement of anti-cancer therapy, as well as growing understanding of the molecular signaling behind cancer, current therapeutic procedures are unreliable (Sobot et al., 2016, Soheilifar et al., 2018). Chemotherapy is the common usual treatment for advanced cancer. However, resistance to chemotherapeutic drugs is the principal limitation of cancer therapy (Lin et al., 2020). One of the main reasons of drug resistance is overexpression of ATP-binding cassette (ABC) transporters (Perla-Lidia et al., 2021). ABC transporters pump chemotherapeutic drugs out of cells, thereby reduce the intracellular concentration of drugs and diminish their anticancer activity (MF Gonçalves et al., 2020).

Therefore, downregulation or inhibition of ABC transporters may enhance the effects of chemotherapeutic agents and made them more efficient in low doses, results in a reduction of chemotherapy side effects. Accumulating evidence shows the positive role of flavonoids in enhancing the efficacy and toxicity of chemotherapy drugs by interaction with the ABC transporters (Li and Paxton, 2013). Galangin (3, 5, 7-trihydroxyflavone) is an Alpinia galangal root extracted flavonoid whose apoptotic effects have been confirmed in different types of cancer (Wen et al., 2020). It is reported that combination use of anticancer drugs with Galangin (GA) amplifies the success of disease management. For example, combination of GA with tumor necrosis factor-related apoptosis-inducing ligand (TRAIL) sensitizes lung cancer cells to TRAIL treatment (Han et al., 2016). Furthermore, it has shown that the presence of GA potentiated the apoptotic effect of Cisplatin against the lung cancer cells (Yu et al., 2018). Despite GA's benefits in cancer therapy, its efficacy has been restricted by low water solubility, lack of oxidative stability, insufficient bioavailability, poor intestinal absorption, and first-pass metabolism (Zhu et al., 2018). Therefore, employing an efficient delivery system may overcome GA's limitations and can broaden its clinical application. Nanoparticle-based drug delivery systems protect the encapsulated drugs from demolition and deliver their cargos to the cancerous cells either via ligands-mediated active targeting or via passive targeting through enhanced permeability and retention (EPR) mechanism (Raj et al., 2019). Recently, Arginyl-glycyl-aspartic acid (RGD) containing nanostructured lipid carrier (NLC-RGD) has been introduced as a suitable drug carrier due to their high loading capacity, improved stability, easy preparation, low toxicity, and targeted delivery (Hajipour et al., 2018, Hajipour et al., 2019). NLCs are relatively new lipid-based delivery systems formed by mixing solid and liquid lipids with aqueous surfactant dispersion (Czajkowska-Kośnik et al., 2021). The efficacy of NLCs can be improved by coating their surface with ligands for specific receptors localized on the cancerous cells (Khajavinia et al., 2012). RGD sequence is recognized by different types of integrins (especially avb3 integrin) and facilitates the uptake of RGD-containing nanoparticles by integrin-mediated endocytosis (Cao et al., 2015, Liu et al., 2017). This investigation aimed to provide GA loaded-NLC-RGD to overcome the therapeutic limitation of GA and evaluate its potential to improve the effects of doxorubicin on the human lung cancer cell line. Moreover, the effects of GA on gene expression of some ABC transporter were studied to discover the probable mechanisms by which GA overcome the drug resistance.

2. Material And Methods

2.1. Materials

Fluorescein dye, Galangin, Dimethyl sulfoxide (DMSO, 99.9%), Fetal Bovine Serum (FBS), 4',6-diamidino-2-phenylindole (DAPI), 3-(4,5-dimethylthiazol-2-yl)-2,5-diphenyltetrazolium bromide (MTT), Phosphate buffered saline, Roswell Park Memorial Institute (RPMI) 1640 Medium and Trypsin (0.25 % EDTA solution) were purchased from Sigma-Aldrich (St. Louis, MO, USA). Glyceryl palmito stearate (Precirol VR ATO 5), DSPE-PEG (2000) amine, and Miglyol were obtained from Gattefosse (St-Priest, France). The human lung carcinoma (A549) cell line was acquired from National Cell Bank, (Pasteur institute, Iran).

2.2. Preparing GA loaded-NLC-RGD

For production of GA loaded-NLC-RGD, hot homogenizer method along with ultra-sonication was used. In this regard, primarily, DSPE-PEG (2000) Amine and RGD were dissolved in DMSO and stirred for 24 h. Next, the mixture was dialyzed against Milli-Q water (membrane tubing, molecular weight cut-off 1000 Da) for 2 days. Then, the final solution was lyophilized to obtain RGD-PEG-DSPE product. In the next step, GA was dissolved in 1 ml ethanol, added into the liquid phase (Miglyol and precirol® ATO 5) at 70°C. The aqueous phase was prepared by dissolving RGD-PEG-DSPE and poloxamer 407 (as surfactant) in water and was added dropwise to the lipid phase under high speed homogenizing at 20,000 rpm speed (Silent Crusher M, Heidolph, Germany) for 18 min. then, the nanoemulsion was sonicated with the frequency of 2 kHz (10 % power, 1 min sonication, and 1 min rest). At last, the oil/water nanoemulsion cooled down at 25°C to allow recrystallization and NLC-RGD production. The products were coded as the A1-A7 with the different compositions of lipids.

2.3. Characterization of GA loaded-NLC-RGD

2.3.1. Particle size, Zeta potential, and Morphology

Samples were diluted with distilled water (1:10) and were assessed using a photon correlation spectroscopy (PCS) (Nano ZS, Malvern Instruments, UK) to determine the particle size and zeta potential by measuring the intensity variations overtime of a laser beam (633 nm).

The morphology of the GA loaded-NLC-RGD particles was revealed via scanning electron microscopy (SEM) (SEM-TESCAN MIRA3-FEG). Samples were dropped on a copper grid and then sputtered with a gold coating before imaging.

2.3.2. Loading capacity and physical stability

To evaluate the encapsulation efficiency (EE) and loading capacity (LC), the UV-visible spectrophotometer (UV160-shimadzo -Japan) was utilized. For this purpose, the calibration curve of GA was plotted according to the concentrations of 5–50 µg/ml. In the next step, the unloaded GA was separated from GA loaded-NLC-RGD by using the Amicon filter (molecular weight cutoff: 30 kDa, Millipore, UK), and optical density of unloaded-GA was measured by UV-visible spectrophotometer at λ_{max} 267 nm. Finally, the concentration of unloaded-GA was calculated based on the calibration curve formula. Following equations were used to calculate the EE and LC.

$$EE(\%) = \frac{\text{concentration}_{\text{total GA}} - \text{concentration}_{\text{free GA}}}{\text{concentation}_{\text{total GA}}} \times 100$$

$$LC\ (mg/g) = \frac{\text{weight}_{\text{loaded GA}}}{\text{weight}_{\text{lipids}}}$$

To evaluate the stability of prepared nanoparticles, GA loaded-NLC-RGD was stored for 2 months at 4–8°C. After this period the particle size and percentage of released GA were assessed.

2.4. Cell viability assay

Human A549 cells were seeded in 96-well plates (10^4 cells/well) and cultivated in RPMI 1640 medium containing 10 % FBS at 37°C in 5 % CO_2 overnight. After the attachment of cells to the plate, they were treated with GA, DOX, and combination of DOX and GA in the free form and loaded in either NLC or NLC-RGD. After 48 h, the cell media were exchanged with 150-µL fresh media including 50 µL of MTT solution (3 mg/mL), and incubated for 4 h at cell culture incubator. Finally, to solve the blue formazan crystals, 175 µL of DMSO and 25 µL Sorensen's glycine buffer were added to each well and optical density (OD) values were recorded at 570 nm using a microplate ELISA reader (ELX 800, Biotek, USA).

2.5. Cellular uptake

To study the cellular uptake, fluorescein was used for labeling the developed nanoparticles. For this purpose, 0.01% w/w fluorescein regarding the weight of the lipids was added to the formulation. Afterward, the unloaded fluorescein was removed by the Amicon® filter (molecular weight cutoff 30 kDa, Millipore, UK) using centrifuging at 4000 rpm for 20 min and washed several times with PBS. A549 cells (3×10^5 cells/mL) were seeded and incubated for 24 h in six-well plate to reach 90% confluence. In the next step, the cells were treated with fluorescein containing NLC with and without RGD for 4 h. Finally, the cells were washed twice with PBS and trypsinized to explore the fluorescein uptake using a FACS Calibur flow cytometer (Becton Dickinson Immunocytometry Systems, San Jose, CA) and fluorescence microscope (Olympus microscope Bh2-RFCA, Japan). To avoid fluorescence dequenching of fluorescein, these experiments were performed in dark.

2.6. Assessment of apoptosis percentage by flow cytometry

Fluorescein isothiocyanate (FITC) labeled annexin V assay was used to determine apoptosis percentage of cells when treated with GA and GA loaded-nanoparticles. For this purpose, A5459 cells were treated with 1 µM DOX, 1 µM DOX + 61 µM GA or equivalent doses of GA loaded nanoparticles. After 24 h, cells were trypsinized, washed, and were incubated with 200 µl of binding buffer containing 5 µl FITC-labeled Annexin V in a dark room for 15 min. Then, 500 µl binding buffer was used to wash the cells. Next, cells were incubated with 200 µl binding buffer containing 5µl propidium iodide (PI) for 5 min at room temperature. Finally, a FACS Calibur flow cytometer (Becton Dickinson Immunocytometry Systems, San Jose, CA) was used to assess the apoptosis and necrosis rate.

2.7. Analysis of apoptotic nuclei by DAPI staining

To analyze, the effects of GA and GA loaded-NLC-RGD on DNA fragmentation and nuclear condensation, the nucleus of A549 cells was stained with DAPI fluorescence dye. In the first step, cells were seeded on coverslip at the density of 4×10^5 per well, then treated with 1 µM DOX + 61 µM GA or equivalent doses of GA loaded nanoparticles at 37°C. After 24 h, cells were washed with PBS and fixed using paraformaldehyde (4%) for 20 min at room temperature. Next, the cells permeabilized using 0.1% (w/v)

Triton X-100 for 15 min and stained with DAPI solution (Sigma, USA) for 40 min in a dark room. Finally, the stained cells were washed twice with cold PBS and the apoptotic morphological alteration of cells was captured using a fluorescence microscope (Bh2-RFCA, Olympus, Japan).

2.8. RNA extraction and analysis of gene expression

Real-time PCR (RT-PCR) was used to assess the effects of GA and GA loaded nanoparticles on the expression of ABCB1, ABCC1, ABCC2, and ABCG2. In brief, A549 cells were treated with either 61 μM GA and GA loaded-NLC-RGD for 48 h. Then, total RNA was extracted by Trizol reagent (Invitrogen Corporation, Carlsbad, California, USA) based on the manufacturer's protocols. Following the RNA quantification by NanoDrop (ND-1000, NanoDrop Technology, Australia), Takara Bio Inc Complementary DNA (cDNA) synthesis Kit was used to cDNA synthesis. Finally, 1μL of each cDNA sample, 1 μL (10 PM/μL) of each primer were mixed with 7 μL of SYBR-Green Master Mix and Real-time PCR (RT-PCR) was run by the Magnetic Induction Cycler (MIC) real-time PCR detection system (BioMolecular Systems, Sydney, Australia). Primer sequences were presented in Table 1. The Pfaffl method was used to normalize the expression of target genes regarding housekeeping gene (GAPDH) expression.

Table 1
Primers sequences

Gene	Forward Primer (5' to 3' direction)	Reverse Primer (5' to 3' direction)	Products size (bp)
ABCB1	TGACAGCTACAGCACGGAAG	TCTTCACCTCCAGGCTCAGT	131
ABCC1	GGGCTGCGGAAAGTCGT	AGCCCTTGATAGCCACGTG	80
ABCC2	TACCAATCCAAGCCTCTACC	AGAATAGGGACAGGAACCAG	104
ABCG2	TTCGGCTTGCAACAACTATG	TCCAGACACACCACGGATAA	128
GAPDH	GACAGTCAGCCGCATCTTCT	TTAAAAGCAGCCCTGGTGAC	127

2.9. Statistical analysis

All of the data were described as the mean ± standard deviation. Statistical analyses were completed using student t-test and ANOVA analyses of variance. Less than 0.05 p-value was considered as significant.

3. Results

3.1. Preparation and characterization of GA loaded-NLC-RGD

The several formulations (Table 2) of GA loaded-NLC-RGD were assessed to reach the optimum characteristic. Based on the size, polydispersity index (PDI), and loading capacity, optimum formulation contained 120 mg Precirol as a central substance of nanoparticles, 15 mg Miglyol as a stabilizer, and 75 mg Poloxamer as a surfactant. As shown in Fig. 1a, mean size of the optimum formulation was 119.4 nm with 0.23 PDI. The result of zeta potential analysis showed that the surface charge of prepared nanoparticles at the original pH 7.4 is -15 mV (Fig. 1b). Scanning electron microscope (SEM) imaging confirmed that prepared nanoparticles have a spherical morphology and nano-sized scale (Fig. 1c). The original data are presented as supplementary file 1, 2 and 3.

Table 2
Composition and characteristics of prepared nanoparticles.

Formulation Code	Precirol mg))	Miglyol (mg)	Poloxamer (mg)	RGD-PEG-DSPE (mg)	Size (nm)	PDI	EE (%)	LC (mg/g)
F1	150	20	80	2	316.2	0.61	89.7 ± 5.3	53.8 ± 3.2
F2	150	15	60	2	281.7	0.47	82.8 ± 5.5	55.2 ± 3.7
F3	150	15	130	2	344.0	0.59	90.2 ± 6.7	45.8 ± 3.4
F4	80	10	80	5	245.1	0.38	80.6 ± 9.0	71.1 ± 7.9
F5	120	20	80	5	138.5	0.21	78.2 ± 9.4	53.3 ± 6.4
F6	120	15	100	5	153.2	0.34	84.2 ± 6.6	53.7 ± 4.2
F7	120	15	75	5	119.4	0.23	83.1 ± 4.3	59.3 ± 3.0

PDI: polydispersity index, EE: encapsulation efficiency, LC: loading capacity, RGD-PEG-DSPE: Arginyl-glycyl-aspartic acid -distearoyl-sn-glycero-phosphoethanolamine-N-[amino (polyethylene glycol)]

3.2. Drug loading and physical stability

Encapsulation efficiency and loading capacity for optimum formulation were calculated 83.1 ± 4.3 % and 59.3 ± 3.0 mg/g respectively. During the 2 months storage at 4–8°C, we observed any significant change in clarity and phase separation of the optimum formulation. Furthermore, the size (127.1 nm) and PDI (0.25) of stored nanoparticles were not significantly different from freshly prepared nanoparticles (Fig. 1d). During this period, less than 10 % of GA were released from NLC-RGD (supplementary file 4).

3.3. Cell viability MTT assay

Cell viability study revealed that IC_{50}s of GA, GA loaded-NLC, GA loaded-NLC-RGD on human lung carcinoma A549 cells are 162.3, 151.0, and 123.4 μM, respectively (Fig. 2a). According to Fig. 2b, DOX inhibits the A549 cell proliferation at IC_{50} of 3.5 μM. These results also showed that, mixture treatment of the A549 cells with 61 μM GA (IC_{20}) + 1 μM DOX, 61 μM GA loaded-NLC + 1 μM DOX and 61 μM GA loaded-NLC-RGD + lμM DOX results in 50.65%, 45.88%, 31.13% cell viability, which indicates that GA loaded-NLC-RGD + DOX is 19.52% and 14.75% more cytotoxic than GA + DOX and GA loaded-NLC + DOX respectively (Fig. 2c and 2e). MTT analyzing data are presented as supplementary file 5.

3.4 Cellular uptake of nanoparticles

Uptake of prepared nanoparticles into cancerous cells was investigated based on the fluorescence intensity of Fluorescein dye using flow cytometry (Fig. 3a) and fluorescent microscope imaging (Fig. 3b). As shown in Fig. 3a, cellular uptake of GA loaded-NLC-RGD is significantly higher than those of GA loaded-NLC, suggesting that RGD facilitates nanoparticle absorption into cells. Fluorescence microscopy imaging confirmed the obtained results from flow cytometry and showed that the fluorescence intensity of cells treated with GA loaded-NLC-RGD was more than those of cells treated with GA loaded-NLC (Fig. 3b). Original data are presented as supplementary file 6.

3.5 Cell apoptosis

Annexin V/PI staining was performed to assess the effects of Galnagin loaded-NLC-RGD on DOX-induced apoptosis in A549 cells. Flow cytometry graphs (Fig. 4a) showed that co-treatment of A549 cells with DOX and GA enhances the apoptosis compared to DOX alone (37.77 % vs 30.0%). Results also confirmed that adjuvant effects of GA loaded-NL-RGD (49.58 %) were higher than GA loaded-NLC (37.36%) and free form of GA (37.77%). The obtained results showed that delivery with NLC-RGD is more capable compared to NLC (supplementary file 7).

3.6 DAPI Staining

Nucleus condensation and chromatin fragmentation of cells as apoptosis signs were compared between cells treated with DOX, DOX + GA, DOX + GA loaded-NLC, and GA loaded-NLC-RGD. DAPI staining confirmed the results of apoptosis experiments and showed that at an equal time and concentration, DOX + GA loaded-NLC-RGD induce DNA degradation more remarkably than DOX + GA and DOX + GA loaded-NLC (Fig. 4b).

3.7 Expression of ABC transporter

To investigate the GA effects on the expression of the ABC transporter family, the mRNA level of important members of the ABC transporter family were assessed in GA treated lung cancer cells. Within each sample, the mRNA level of each gene was normalized to GAPDH mRNA level, as a housekeeping gene. As shown in Fig. 5 (a, b, c), treatment of A549 lung cancer cells with GA or GA loaded-NLC-RGD, downregulate the expression of ABCB1, ABCC1, and ABCC2 in comparison with the untreated group

(control). However, we didn't find any alteration in the expression of ABCG2, when cells were treated either with the GA or GA loaded-NLC-RGD (Fig. 5d). These results also demonstrated that the effect of GA loaded-NLC-RGD on downregulation of ABCB1, ABCC1, and ABCC2 is more than GA (supplementary file 8).

4. Discussion

The present study confirmed that the GA loaded-NLC-RGD could significantly improve the anticancer potential of DOX. Previously synergistic effects of Gallatin and the chemotherapeutic agents have been reported in cancer treatment (Ren et al., 2016, Yu et al., 2018). However, low bioavailability and flavonoid first-pass metabolism attenuate the anticancer effects of GA (Wu et al., 2011, Zhu et al., 2018). Based on our results, NLC-RGD is an appropriate carrier for delivering GA into the adenocarcinoma human alveolar basal epithelial cells. Nanoparticles in a size range of 30–200 nm are suitable for drug delivery (Hajipour et al., 2021). Nanoparticles larger than 30 nm are easily omitted by the reticuloendothelial system, and those smaller than 20 nm are removed by renal excretion (Hajipour et al., 2018). Zeta potential as an indicator of nanoparticle surface charge controls the repulsive force among nanoparticles and the stability of the drug delivery system (Hufschmid et al., 2019). It is also reported that neutral or faintly negative ZP is more compatible to interact with the cell membrane (Lane et al., 2015). The Zeta potential of prepared nanoparticles is high enough to provide acceptable stability, and also is not too negative to prevent nanoparticles and cell membrane interaction.

To develop targeted nanoparticles, RGD was added to the formulation that can deliver the drug directly to a cancer cell by binding to integrins. Given to overexpression of αvβ3 and αvβ6 integrin on the surface of the A549 lung cancer cells (Heikkilä et al., 2009), the presence of RGD in NLC formulation increases the cellular uptake of nanoparticles and enhances their therapeutic efficiency (Yoo et al., 2019). Furthermore, overexpression of integrins (RGDs receptors) in vascular endothelial cells of tumor tissue, makes RGD a well-known tumor-targeting peptide (Nieberler et al., 2017). Moreover, given the key role of integrins in cell adhesion and cancer development, RGD containing nanoparticles can inhibit metastasis by blocking the integrins (Hajipour et al., 2019). Comparison accumulation of NLC with NLC-RGD in the cell in uptake experiments established that RGD containing nanoparticles have a great binding affinity to cancerous cells. Due to the in-vitro nature of our study, all beneficial aspects of nanoparticle delivery systems were not observable. In in-vivo systems, NLC-RGD not only deliver their cargo by RGD mediated active targeting, but also provide the drug accumulation into tumor tissue by EPR mediated passive targeting (Kang et al., 2020). In addition, in in-vivo systems nanoparticles are absorbed by Peyer's patches (M cells) in the small intestine, which results in bypassing the liver and therefore decrease first-pass metabolism (Kakran et al., 2011).

Cell viability and apoptosis experiments showed that co-treatment of A549 cells with GA and DOX is more toxic and more apoptotic compared to DOX. These observations are in accordance with previous studies, which reported that GA prevents cancer development by reversal of the Warburg effect (Ji et al., 2019), motivate reactive oxygen species (ROS) mediated apoptosis, or the mitochondrial-dependent apoptosis

pathway (Zhang et al., 2012), G0/G1 phase cell cycle arrest (Gwak et al., 2011), and inhibition of multidrug resistance (MDR) (Lorendeau et al., 2014). In this regard, Yu et al. (Yu et al., 2018) showed that GA decreases the Cisplatin resistance of human lung cancer cells and potentiates apoptosis via Bcl-2 suppression. Inactivating Akt and promoting the Caspase-3 pathway are other mechanisms by which GA inhibits retinoblastoma cell proliferation (Zou and Xu, 2018). Given to Over-expression of specific ABC transporters in several types of cancers and their roles in tumor-initiating (Muriithi et al., 2020), the main aim of this study was to investigate the expression of ABC transporter under the influence of GA loaded NLC-RGD. Downregulation or inhibition of the ABC transporter sensitizes cancer cells to chemotherapeutic agents (Nanayakkara et al., 2018). To our knowledge, this is the first study that reports the downregulation of ABCB1, ABCC1, and ABCC2 as another mechanism by which GA enhances the apoptotic effects of DOX. However, in the opposite of these results, Critchfield et al. (Critchfield et al., 1994) reported that GA stimulates P-glycoprotein efflux of adriamycin in HCT-15 colon carcinoma cells. There is no logical interpret for this controversial report. Our experiments also revealed that the effects of GA on the expression of ABC transporter were strengthened when used in the form of GA loaded-NLC-RGD, confirming the appropriateness of prepared nanoparticles. Results showed that improved targeting of GA makes the DOX more effective for apoptosis induction. Therefore, low doses of DOX can be more effective for cancer inhibition, which in turn decreases the side effects of DOX.

Conclusion

NLC-RGD is a suitable drug delivery system to convey GA into cancerous cells due to appropriate delivery characteristics and specialized RGD mediated uptake mechanism. The potential of GA in downregulation of ABC transporter leads to an increase of anticancer effects of chemotherapeutic drugs such as DOX. Therefore, overcoming the therapeutic limitation of GA by NLC-RGD as a nanoparticle delivery system makes it an effective adjuvant to enhance the efficacy of chemotherapeutic agents in cancer therapy.

Declarations

Acknowledgment

Thanks to guidance and advice from "Clinical Research Development Unit of Baqiyatallah Hospital".

Ethical Approval

Procedure of study was approved by the Ethical Committee of Baqiyatallah University of Medical Sciences (IR.BMSU.REC.1399.202).

Consent to Participate

Not applicable

Consent to Publish

Not applicable

Authors Contributions

HH, RT and MG conceived and designed research. HH, MN and MG conducted experiments. MN and RZE provided setups and reagents/samples. AB and RZE analyzed data. HH and AB wrote the manuscript. MG revised the manuscript. RT supervised the study. All authors read and approved the manuscript and all data were generated in-house and that no paper mill was used.

Funding

Project supported by Nanobiotechnology Research Center of Baqiyatallah University of Medical Sciences (project number: 98000453, IR.BMSU.REC.1399.202).

Competing Interests

The authors confirm that they have no conflict of interest

Availability of data and materials

Data generated during this study are included in supplementary material.

References

1. Cao Y, Zhou Y, Zhuang Q, Cui L, Xu X, Xu R, He X (2015) Anti-tumor effect of RGD modified PTX loaded liposome on prostatic cancer. Int J Clin Exp Med 8:12182
2. Critchfield JW, Welsh CJ, Phang JM, Yeh GC (1994) Modulation of adriamycin® accumulation and efflux by flavonoids in HCT-15 colon cells: activation of P-glycoprotein as a putative mechanism. Biochem Pharmacol 48:1437–1445
3. Czajkowska-Kośnik A, Szymańska E, Czarnomysy R, Jacyna J, Markuszewski M, Basa A, Winnicka K (2021) Nanostructured Lipid Carriers Engineered as Topical Delivery of Etodolac: Optimization and Cytotoxicity Studies. Materials 14:596
4. Gwak J, Oh J, Cho M, Bae SK, Song I-S, Liu K-H, Jeong Y, Kim D-E, Chung Y-H, Oh S (2011) Galangin suppresses the proliferation of β-catenin response transcription-positive cancer cells by promoting adenomatous polyposis coli/Axin/glycogen synthase kinase-3β-independent β-catenin degradation. Mol Pharmacol 79:1014–1022
5. Hajipour H, Farzadi L, Roshangar L, Latifi Z, Kahroba H, Shahnazi V, Hamdi K, Ghasemzadeh A, Fattahi A, Nouri M (2021) A human chorionic gonadotropin (hCG) delivery platform using engineered uterine exosomes to improve endometrial receptivity. Life Sciences: 119351
6. Hajipour H, Ghorbani M, Kahroba H, Mahmoodzadeh F, Emameh RZ, Taheri RA (2019) Arginyl-glycyl-aspartic acid (RGD) containing nanostructured lipid carrier co-loaded with doxorubicin and sildenafil citrate enhanced anti-cancer effects and overcomes drug resistance. Process Biochem 84:172–179

7. Hajipour H, Hamishehkar H, Nazari Soltan Ahmad S, Barghi S, Maroufi NF, Taheri RA (2018) Improved anticancer effects of epigallocatechin gallate using RGD-containing nanostructured lipid carriers. Artificial Cells Nanomedicine Biotechnology 46:283–292
8. Han MA, Lee DH, Woo SM, Seo BR, Min K-j, Kim S, Park J-W, Kim SH, Choi YH, Kwon TK (2016) Galangin sensitizes TRAIL-induced apoptosis through down-regulation of anti-apoptotic proteins in renal carcinoma Caki cells. Scientific reports 6:1–10
9. Heikkilä O, Susi P, Stanway G, Hyypiä T (2009) Integrin αVβ6 is a high-affinity receptor for coxsackievirus A9. J Gen Virol 90:197–204
10. Hufschmid R, Teeman E, Mehdi BL, Krishnan KM, Browning ND (2019) Observing the colloidal stability of iron oxide nanoparticles in situ. Nanoscale 11:13098–13107
11. Ji X, Lu Y, Tian H, Meng X, Wei M, Cho WC (2019) Chemoresistance mechanisms of breast cancer and their countermeasures. Biomed Pharmacother 114:108800
12. Kakran M, Sahoo N, Li L (2011) Dissolution enhancement of quercetin through nanofabrication, complexation, and solid dispersion. Colloids Surf B 88:121–130
13. Kang H, Rho S, Stiles WR, Hu S, Baek Y, Hwang DW, Kashiwagi S, Kim MS, Choi HS (2020) Size-dependent EPR effect of polymeric nanoparticles on tumor targeting. Advanced healthcare materials 9:1901223
14. Khajavinia A, Varshosaz J, Dehkordi AJ (2012) Targeting etoposide to acute myelogenous leukaemia cells using nanostructured lipid carriers coated with transferrin. Nanotechnology 23:405101
15. Lane LA, Qian X, Smith AM, Nie S (2015) Physical chemistry of nanomedicine: understanding the complex behaviors of nanoparticles in vivo. Annu Rev Phys Chem 66:521–547
16. Li Y, Paxton JW (2013) The effects of flavonoids on the ABC transporters: consequences for the pharmacokinetics of substrate drugs. Expert Opin Drug Metab Toxicol 9:267–285
17. Lin KH, Rutter JC, Xie A, Pardieu B, Winn ET, Dal Bello R, Forget A, Itzykson R, Ahn Y-R, Dai Z (2020) Using antagonistic pleiotropy to design a chemotherapy-induced evolutionary trap to target drug resistance in cancer. Nat Genet 52:408–417
18. Liu R, Li X, Xiao W, Lam KS (2017) Tumor-targeting peptides from combinatorial libraries. Adv Drug Deliv Rev 110:13–37
19. Lorendeau D, Dury L, Genoux-Bastide E, Lecerf-Schmidt F, Simões-Pires C, Carrupt P-A, Terreux R, Magnard S, Di Pietro A, Boumendjel A (2014) Collateral sensitivity of resistant MRP1-overexpressing cells to flavonoids and derivatives through GSH efflux. Biochem Pharmacol 90:235–245
20. MF Gonçalves B, Cardoso SP, U Ferreira D M-J (2020) Overcoming Multidrug Resistance: Flavonoid and Terpenoid Nitrogen-Containing Derivatives as ABC Transporter Modulators. Molecules 25:3364
21. Muriithi W, Macharia LW, Heming CP, Echevarria JL, Nyachieo A, Niemeyer Filho P, Neto VM (2020) ABC transporters and the hallmarks of cancer: roles in cancer aggressiveness beyond multidrug resistance. Cancer Biology Medicine 17:253

22. Nanayakkara AK, Follit CA, Chen G, Williams NS, Vogel PD, Wise JG (2018) Targeted inhibitors of P-glycoprotein increase chemotherapeutic-induced mortality of multidrug resistant tumor cells. Scientific reports 8:1–18
23. Nieberler M, Reuning U, Reichart F, Notni J, Wester H-J, Schwaiger M, Weinmüller M, Räder A, Steiger K, Kessler H (2017) Exploring the role of RGD-recognizing integrins in cancer. Cancers 9:116
24. Perla-Lidia P-P, Stephanie-Talia M-M, Mónica-Griselda A-M, Luz-María T-E (2021) ABC transporter superfamily. An updated overview, relevance in cancer multidrug resistance and perspectives with personalized medicine. Molecular biology reports: 1–19
25. Raj S, Khurana S, Choudhari R, Kesari KK, Kamal MA, Garg N, Ruokolainen J, Das BC, Kumar D (2019) Specific targeting cancer cells with nanoparticles and drug delivery in cancer therapy. In: Seminars in cancer biology. Elsevier
26. Ren K, Zhang W, Wu G, Ren J, Lu H, Li Z, Han X (2016) Synergistic anti-cancer effects of galangin and berberine through apoptosis induction and proliferation inhibition in oesophageal carcinoma cells. Biomed Pharmacother 84:1748–1759
27. Sobot D, Mura S, Couvreur P (2016) How can nanomedicines overcome cellular-based anticancer drug resistance? Journal of Materials Chemistry B 4:5078–5100
28. Soheilifar MH, Taheri RA, Emameh RZ, Moshtaghian A, Kooshki H, Motie MR (2018) Molecular Landscape in Alveolar Soft Part Sarcoma: Implications for Molecular Targeted Therapy. Biomed Pharmacother 103:889–896
29. Wen SY, Chen JY, Chen CJ, Huang CY, Kuo WW (2020) Protective effects of galangin against H2O2-induced aging via the IGF-1 signaling pathway in human dermal fibroblasts. Environmental toxicology 35:115–123
30. Wu B, Kulkarni K, Basu S, Zhang S, Hu M (2011) First-pass metabolism via UDP-glucuronosyltransferase: a barrier to oral bioavailability of phenolics. Journal of pharmaceutical sciences 100:3655–3681
31. Yoo J, Park C, Yi G, Lee D, Koo H (2019) Active targeting strategies using biological ligands for nanoparticle drug delivery systems. Cancers 11:640
32. Yu S, Gong L-s, Li N-f, Pan Y-f, Zhang L (2018) Galangin (GG) combined with cisplatin (DDP) to suppress human lung cancer by inhibition of STAT3-regulated NF-κB and Bcl-2/Bax signaling pathways. Biomed Pharmacother 97:213–224
33. Zhang H-T, Wu J, Wen M, Su L-J, Luo H (2012) Galangin induces apoptosis in hepatocellular carcinoma cells through the caspase 8/t-Bid mitochondrial pathway. Journal of Asian natural products research 14:626–633
34. Zhu J, Wang Q, Li H, Zhang H, Zhu Y, Omari-Siaw E, Sun C, Wei Q, Deng W, Yu J (2018) Galangin-loaded, liver targeting liposomes: Optimization and hepatoprotective efficacy. Journal of Drug Delivery Science Technology 46:339–347
35. Zou W-W, Xu S-P (2018) Galangin inhibits the cell progression and induces cell apoptosis through activating PTEN and Caspase-3 pathways in retinoblastoma. Biomed Pharmacother 97:851–863

Figures

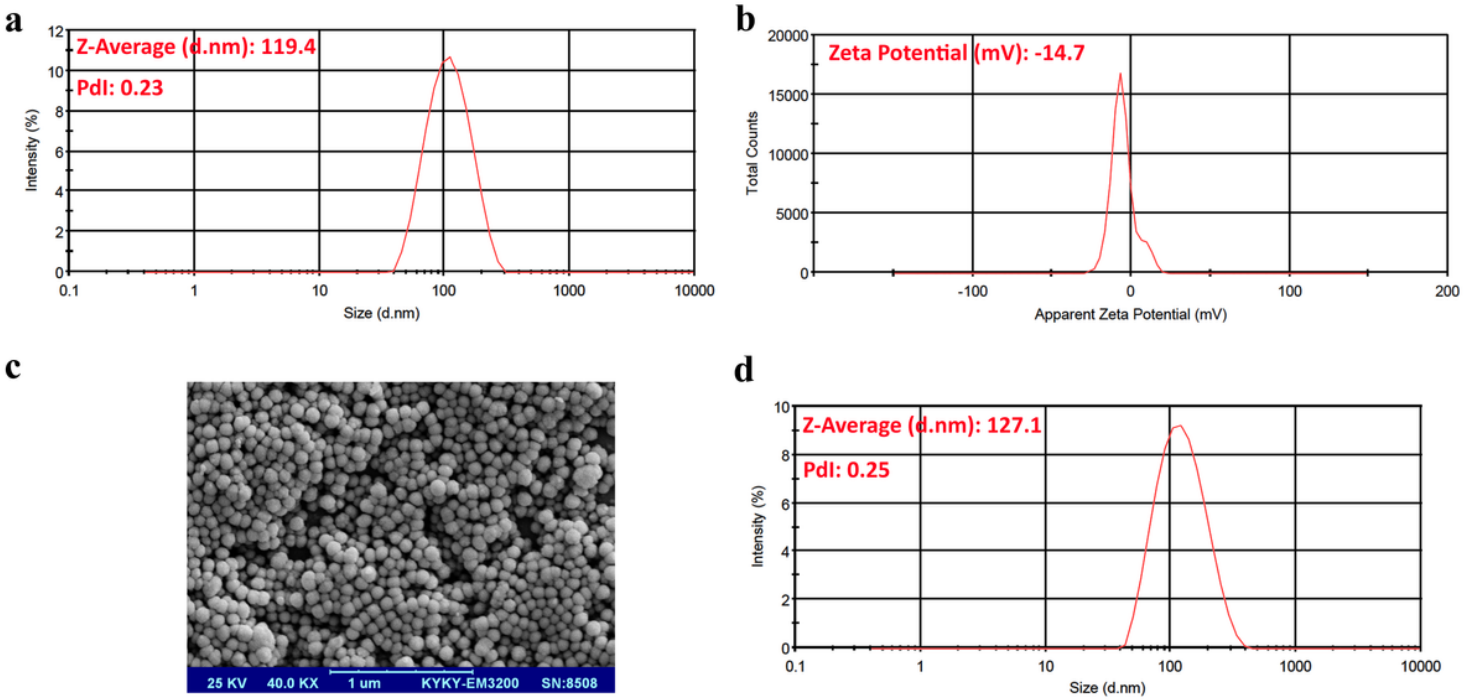

Figure 1

Characteristics of GA loaded-NLC-RGD. a) Size and polydispersity index (PDI) of freshly prepared nanoparticles, b) Zeta potential distribution of GA loaded-NLC-RGD, c) Transmission Electron Microscopy (TEM) image of nanoparticles, d) Size and polydispersity index (PDI) of GA loaded-NLC-RGD after 2 months storage at 4-8 °C. (GA, Galangin; NLC-RGD, Arginyl-glycyl-aspartic acid-containing nanostructured lipid carriers).

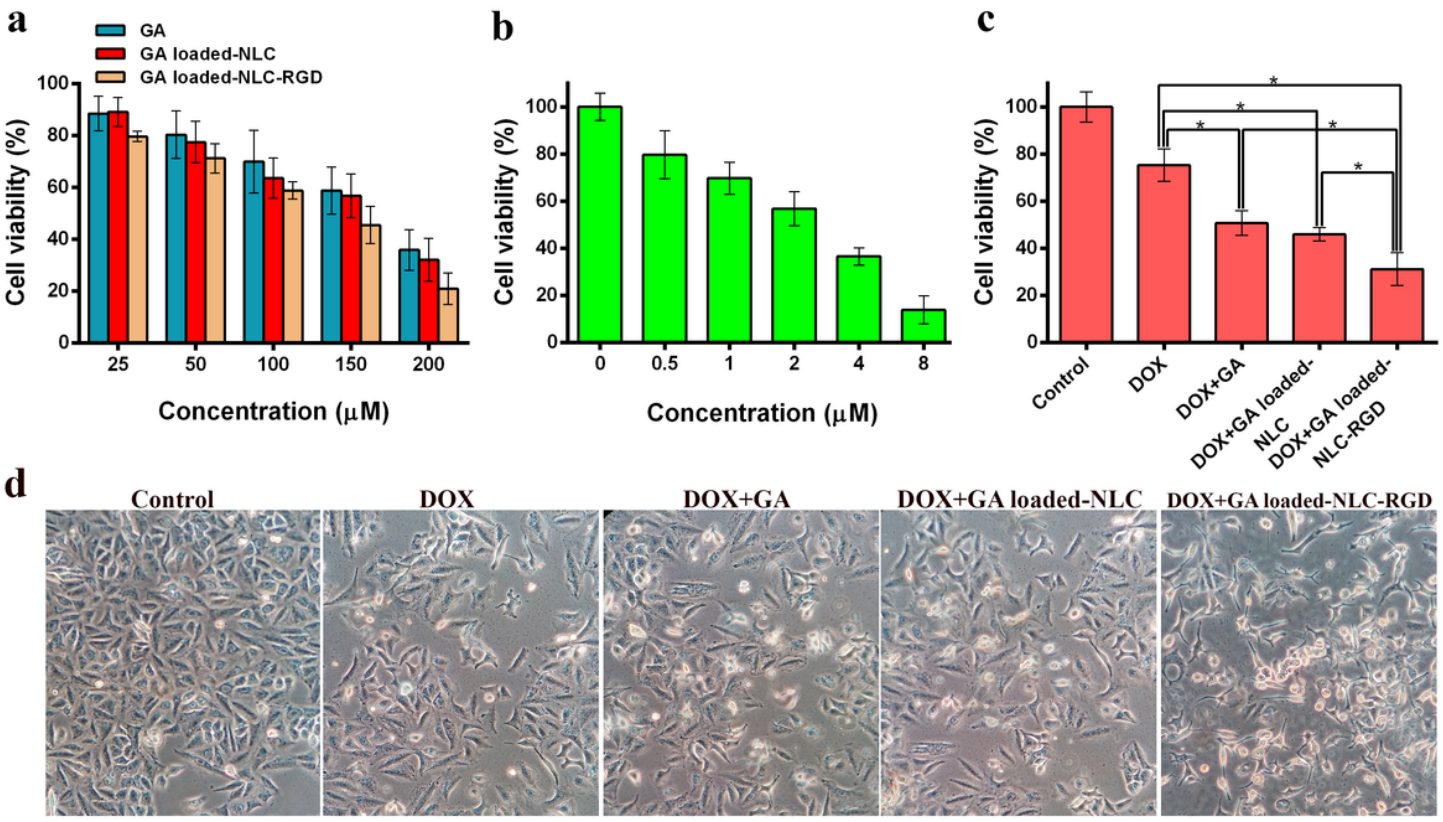

Figure 2

Cell viability of human lung cancer cells (A549) after 48 h treatment with (a) GA and GA loaded nanoparticles, (b) Diverse concentration of doxorubicin, (c) Combination of 1μM DOX and 61 μM GA in free form and the form of loaded NLC and NLC-RGD. d) Phase-contrast image of cells when treated with DOX and GA in free form and the form of loaded nanoparticles. Data are presented as mean ± standard deviation (n=3) and asterisk indicates significant differences between two groups at p <05. (DOX, Doxorubicin; GA, Galangin; NLC, nanostructured lipid carriers; NLC-RGD, Arginyl-glycyl-aspartic acid-containing nanostructured lipid carriers).

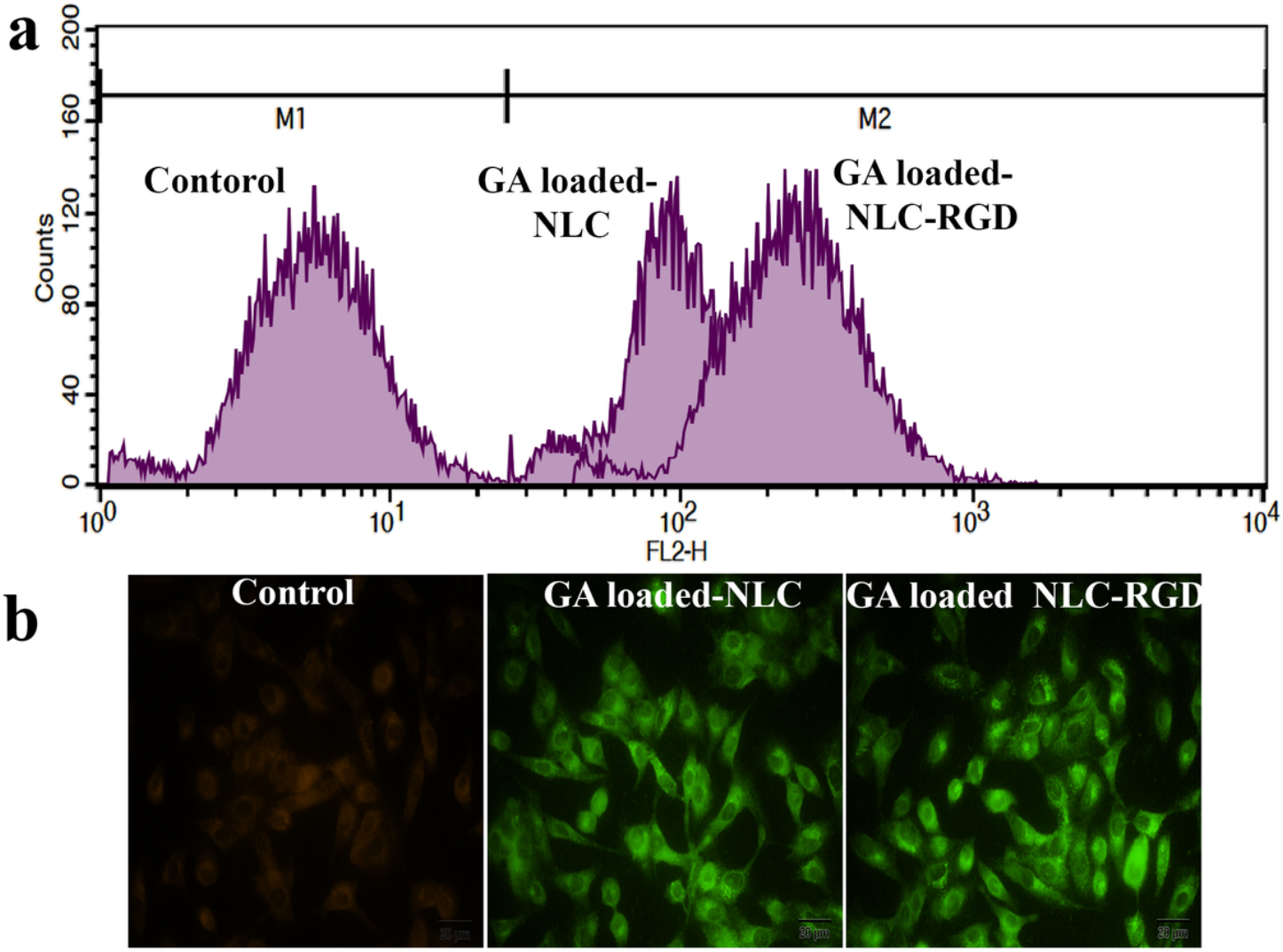

Figure 3

Cell uptake study of NLC versus NLC-RGD. a) Fluorescence intensity graphs of fluorescein loaded NLC and NLC-RGD. b) Fluorescent microscope imaging of A549 cells after 4 h incubation with fluorescein-loaded NLC and NLC-RGD. (NLC, nanostructured lipid carriers; NLC-RGD, Arginyl-glycyl-aspartic acid-containing nanostructured lipid carriers).

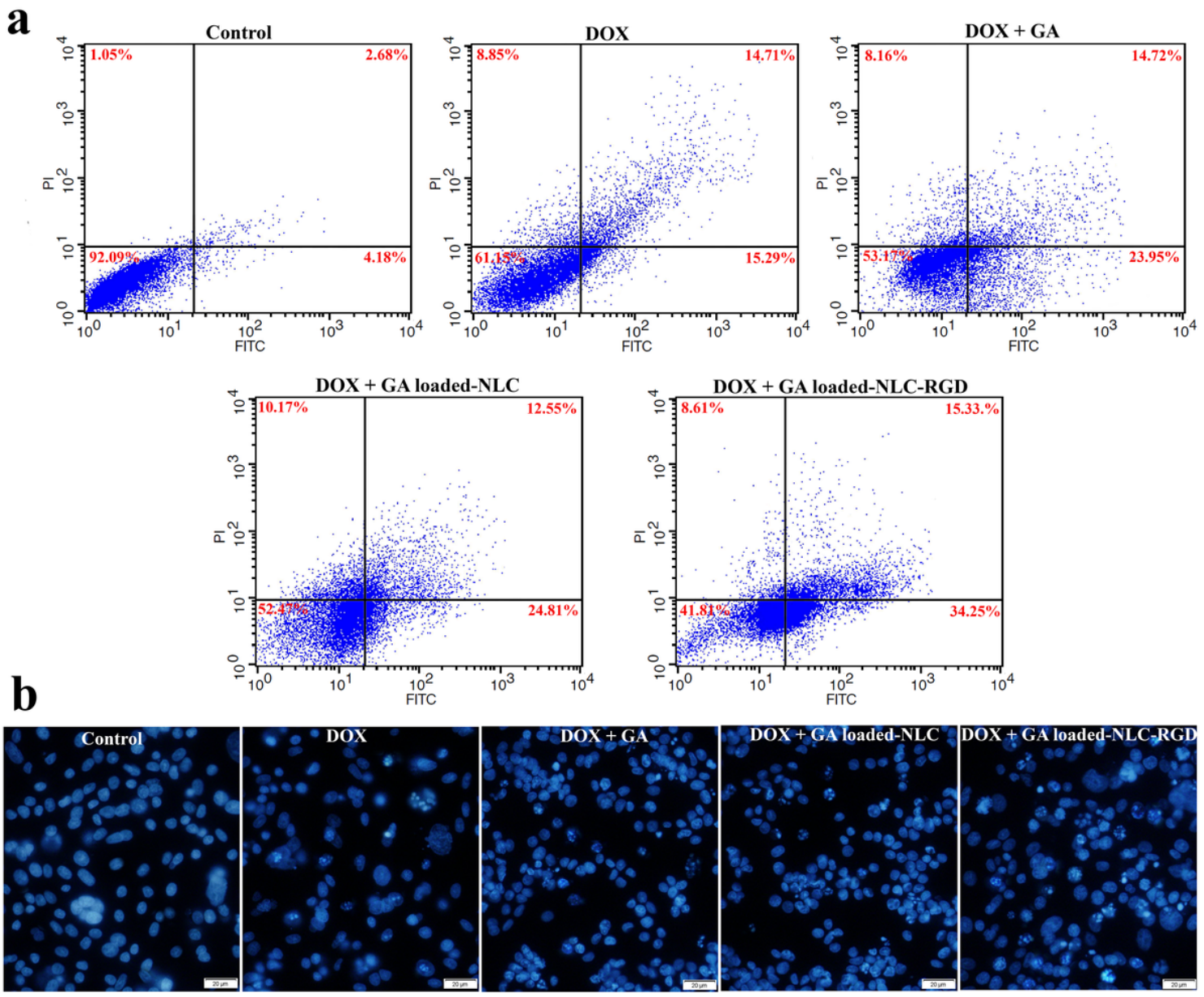

Figure 4

a) Apoptosis flow cytometry graphs of A549 cell when treated with DOX and GA in the free from and the form of loaded NLC and NLC-RGD. Each graph shows the percentage of viable cells (bottom left quadrant), early apoptotic cells (bottom right quadrant), late apoptotic cells (top left quadrant), and necrotic cells (top right quadrant). b) DAPI stained cancerous cells following 48 h treatment of cells with DOX and GA in the free from and the form of loaded into NLC and NLC-RGD. (DOX, Doxorubicin; GA, Galangin; NLC, nanostructured lipid carriers; NLC-RGD, Arginyl-glycyl-aspartic acid-containing nanostructured lipid carriers).

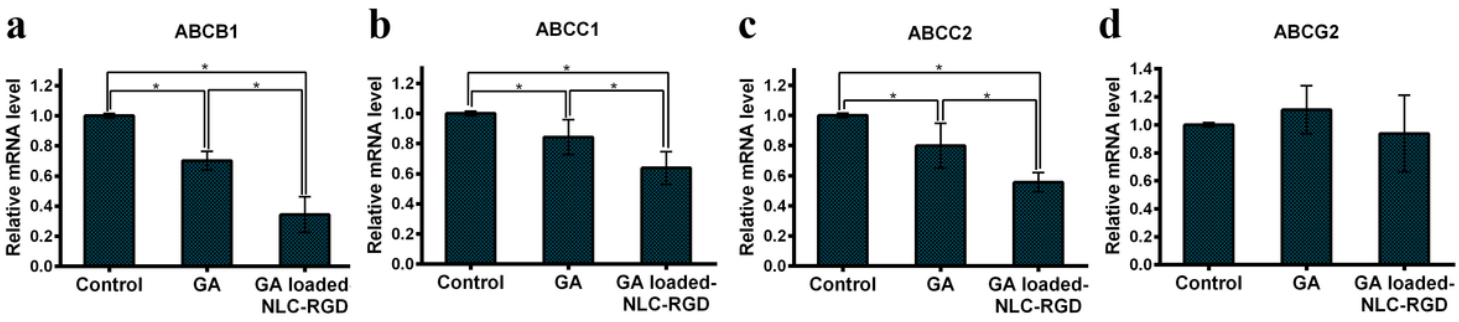

Figure 5

Effects of GA and GA-loaded-NLC-RGD on the expression of ABC transporters genes (ABCB1, ABCC1, ABCC2, and ABCG2) in human lung cancer cells. The effect of GA on downregulation of ABCB1, ABCC1, and ABCC2 is intensified when used in the form of GA loaded-NLC-RGD. Neither GA nor GA loaded-NLC-RGD alters the expression level of ABCG2. The results were considered as the mean ± standard deviation (n=3) and asterisk indicates significant differences between two groups at p <05. (GA, Galangin; NLC-RGD, Arginyl-glycyl-aspartic acid-containing nanostructured lipid carriers).

Supplementary Files

This is a list of supplementary files associated with this preprint. Click to download.

- supplementaryfile1.pdf
- supplementaryfile2.pdf
- supplementaryfile3.pdf
- supplementaryfile4.pdf
- supplementaryfile5.xlsx
- supplementaryfile6.pdf
- supplementaryfile7.pdf
- supplementaryfile8.xlsx